Self-Consistent Field Investigation of Pattern-Forming Electroneutral Blends of Charged Polymers

Wai-Ming Tam and Galen T. Pickett*

Department of Physics and Astronomy, California State University Long Beach, 1250 Bellflower Boulevard, Long Beach, California 90840

Received August 23, 2002. In Final Form: December 3, 2002

Electroneutral blends of oppositely and uniformly charged flexible polymers spontaneously microsegregate, recapitulating phases formed in block copolymer melts. The length scale of the pattern is controlled by the charge density and the thermodynamic incompatibility of two species, with the molecular weight of the chains entering as a small correction. We calculate the disordered phase spinodal in the random phase approximation and determine the microphase diagrams numerically for the disordered−cylindrical−lamellar phases in a two-dimensional self-consistent lattice model. The mesophases are intrinsically characterized by spontaneous charge separation, so the morphology and orientation of the patterned phases are quite sensitive to externally applied electric fields.

1. Introduction

Self-assembly of complex patterns is possible through just a handful of simple interactions operating on relatively simple constituents.[1] The ultimate expression of this is perhaps biological, where steric, electrostatic, solvophilic/phobic, and hydrogen bonding interactions acting among linked amino acids give rise to the ultimate functionality of the tertiary structure of folded proteins,[2] not to mention fully functioning organisms themselves. While self-assembled patterns of biological complexity are not the focus of this paper, it is worth noting that biologically inspired strategies for self-assembly are continually being harnessed in engineering contexts to create materials with novel and desired properties.

A highly studied instance of this paradigm is the case of the block copolymers. The simplest of these molecules, the diblock copolymers, resemble small molecule surfactants, or even the constituents of cell membranes. The molecule is formed by a long block of one type of monomer, say A, connected to a long block of B type monomers. The intrinsic thermodynamic incompatibility of these monomers can be used to drive the formation of membranes[3] in blend-compatibilization and strengthening applications.[4] Additionally, in the neat, melt state, these molecules form a variety of phases with a microscopic pattern, whose symmetry and length scale depend on both the number of A and B monomers on a single chain and the temperature-scaled exchange interaction, the χ parameter of Flory. These three-dimensional microphases can be quite complicated in the bulk[5] but are even more interesting when confined into thin films where the interactions between the film thickness-induced confinement, surface interactions, and the natural pattern length scale combine to produce patterns with a controllable nanoscopic length scale.[6,7] These patterned films are being used in the creation of large arrays of magnetic and superconducting dots and as optoelectronic devices.[8]

While a full theoretical picture of the ordering mechanisms and the thermodynamic phases of these bulk patterns has been developed based upon the self-consistent field approach,[5,9] earlier treatments of the problem suggest a novel means of creating diblocklike patterns in *blends of homopolymers*. The technological, theoretical, and practical advantages to working with homopolymer blends are substantial. Homopolymers are chemically much simpler than diblocks, with a consequently smaller price tag to produce in economically significant volumes. The fact that each chain has a single kind of monomer attached to it greatly simplifies the analysis of their equilibrium thermodynamics, and without the strong AB covalent bond holding the blocks together, a blend is considerably more processable than its diblock analogue.

In the mid-1980s, a coarse-grained, tractable field theory replicating many of the properties of the diblock melt was discovered.[10] Initially by addition of a trivial term to the Cahn−Hilliard dynamical equation for a phase-separating mixture, textures very similar to those produced by diblocks were observed in numerical experiments. When a short-ranged repulsion between components (roughly describing the contacts between monomers of different types and controlled by the χ parameter) is balanced with a long-ranged *attraction* between the two components, many of the diblock phases result. If we let $\phi(\vec{r})$ stand for the local volume fraction of A monomers in excess of their average value, the order-parameter-conserving dynamics leading to pattern formation is governed by the following equation:[11]

$$\partial_t \phi = \nabla^2(t\phi + \phi^3 - k\nabla^2\phi) - B\phi \qquad (1)$$

With $B = 0$, this equation is capable of following the spinodal decomposition of a binary blend of A and B homopolymers. The parameter t is related to the Flory

(1) Peters, R. D.; Yang, X. M.; Wang, Q.; de Pablo, J. J.; Nealey, P. F. *J. Vac. Sci. Technol., B* **2000**, *18*, 3530.
(2) Onuchic, J. N.; Luthey-Schulten, Z.; Wolynes, P. G. *Annu. Rev. Phys. Chem.* **1997**, *48*, 545.
(3) Discher, B. M.; Won, Y.-Y.; Ege, D. S.; Lee, J. C.-M.; Bates, F. S.; Discher, D. E.; Hammer, D. A. *Science* **1999**, *284*, 1143.
(4) Mathur, D.; Nauman, E. B. *J. Appl. Polym. Sci.* **1999**, *72*, 1151.
(5) Matsen, M. W.; Bates, F. S. *Macromolecules* **1996**, *29*, 1091.
(6) Walton, D. G.; Kellog, G. J.; Mayes, A. M.; Lambooy, P.; Russell, T. P. *Macomolecules* **1994**, *27*, 6225.
(7) Kellogg, G. J.; Walton, D. J.; Mayes, A. M.; Lambooy, P.; Russell, T. P.; Gallagher, P. D.; Satija, S. K. *Phys. Rev. Lett.* **1996**, *76*, 2503.
(8) Park, M.; Harrison, C.; Chaikin, P. M.; Register, R. A.; Adamson, D. H. *Science* **1997**, *276*, 1401.
(9) Drolet, F.; Fredrickson, G. H. *Phys. Rev. Lett.* **1999**, *83*, 4317.
(10) Ohta, T.; Kawasaki, K. *Macromolecules* **1986**, *19*, 2621.
(11) Hohenberg, P. C.; Halperin, B. I. *Rev. Mod. Phys.* **1977**, *49*, 435.

10.1021/la026465f CCC: $25.00
Published on Web 01/21/2003

parameter and the molecular weight of the A and B chains (assumed both to have N monomers) by $t = (1 - \chi N/2)$, so that $t = 0$ corresponds to the phase separation point, and $t > 0$ causes the blend to be in the uniformly mixed phase. The addition of the B term, however, was found to halt the growth of domains during spinodal decomposition, leading to a well-defined pattern length scale. Interestingly, this equation of motion can be derived from a free energy functional for the diblocks:

$$F_{\text{coarse-grained}} = \left(\int \mathrm{d}^3 r \frac{t}{2}\phi^2 + \frac{1}{4}\phi^4 + \frac{k}{2}\nabla\phi\cdot\nabla\phi \right) + \frac{B}{2}\int \mathrm{d}^3 r\, \mathrm{d}^3 r' \phi(r) G(r, r') \phi(r') \quad (2)$$

where the long-ranged attraction interaction kernel $G(r, r')$ satisfies[10]

$$\nabla_r^2 G(r, r') = -\delta(r - r') \quad (3)$$

Thus, the long-range interaction responsible for the establishment of order in this model has exactly the form of the usual *electrostatic* interaction for a mixture of oppositely charged, thermodynamically incompatible fluids. Formally, the order parameter ϕ results in the creation of a charge density field:

$$\rho_{\text{es}} = \sqrt{B}\phi \qquad \text{with } -\nabla^2 \Phi_{\text{es}} = \rho_{\text{es}} \quad (4)$$

where the electrostatic potential Φ_{es} is related to the order parameter through

$$\Phi_{\text{es}}(\vec{r}) = \int \mathrm{d}^3 r' G(r, r') \phi(r') \quad (5)$$

Conventionally, positive values of ϕ will correspond to a local excess of A monomers and an "effective" positive charge density, while a local excess of B monomers leads to a negative charge density. Thus, macroscopic phase separation driven by $t < 0$ (that is, $\chi N > 2$) cannot occur, as separating opposite "charges" macroscopically can be made to cost an arbitrarily large free energy simply by letting the overall system size become larger and larger.

While not replicating the most important features of real diblock copolymers (for example, how monodispersity affects the structure of the microsegregated domains[12,25]), the electric field lines generated by a nonuniform ϕ loosely correspond to the actual trajectories of the stretched blocks of the copolymers. The electrostatic analogy for the local Gaussian stretching cost for a nonuniformly stretched polymer is at the root of the first successful calculations on polymer brushes by Semenov.[12] Earlier attempts to get at the correct scaling of the strongly segregated diblock free energy[13,14] can be cast into an electrostatics language,[15,16] whereby the source of charge is identified not with the concentration of A over B monomers but by the concentration of *free ends*. The electrostatic analogy can never be entirely exact, as the monodispersity of the chains imposes a constraint (in fact, a very harsh one that determines the basic structure of the brush or copolymer domains in the classical limit) on the electric field that can be satisfied only when the electric field has a nonzero curl. In some respects, an incompressible, inviscid fluid analogy is more appropriate.[17,18]

At any rate, given the fact that the electrostatic analogy is so successful in reproducing, albeit in a very rough and general way, the features of chain conformation, stretching, incompatibility, and covalent bonding, it is tempting to take the electrostatic analogy *at face value* and honestly calculate the properties of a polymeric blend characterized by *genuine* opposite electric charges. Thus, we will examine the pattern-forming possibilities in an overall neutral blend of oppositely charged polymers. Here, the electric field will be a genuine physical static field with zero curl and will reflect not a sketchy approximation of the local chain conformations but rather the interaction of genuine electric charges embedded into the chemical composition of the two components of the blend.

This is far from the first suggestion that blends of oppositely charged polymers can form microphases, either in the bulk[19−22] or through surface driving forces.[23] Also, layering of oppositely charged polymers is kinetically possible through the layer-by-layer assembly technique.[24] What is new, and supported by the numerical self-consistent field (SCF) calculations below,[26] is the conclusion that many block copolymer results are directly applicable to the present system. In particular, the SCF formalism allows an investigation away from both the strong and weak segregation regimes.

The paper is organized as follows. Initially, we will determine the limit of linear stability of the electroneutral weakly charged blend in the random phase approximation (RPA). Then, a simple calculation in the sharp-interface, strong segregation limit will locate the phase boundaries of the lamellar−cylindrical transition and the disordered−spherical transition. We will then describe how electrostatics has been incorporated into the SCF calculation and bring the results of all these calculations together. After discussing these results and their implications for field-induced control of surface patterns, we draw our conclusions.

2. Random Phase Approximation

For simplicity's sake, let us consider a blend of two homopolymers, type A and B, both having the same number of monomers on them, N. In the incompressible blend, let f stand for the volume fraction of the blend composed of A monomers, so that the volume fraction of B monomers is $(1 - f)$. Thus, f controls the overall composition of the blend, as a similar parameter controls the *composition asymmetry* of a conventional diblock. Thus, $f = 1/2$ characterizes a 50−50 blend of A and B chains. Let us suppose that A monomers have on average ρ_{A} units of electric charge and B monomers carry ρ_{B} units of charge. We assume that individual chains are so lightly charged that their melt conformations are weakly per-

(12) Semenov, A. N. *Sov. Phys. JTEP* **1985**, *61*, 733.
(13) Alexander, S. *J. Phys.* (*Paris*) **1977**, *38*, 983.
(14) deGennes, P.-G. *J. Phys.* (*Paris*) **1976**, *36*, 1443.
(15) Fredrickson, G. H.; Ajdari, A.; Leibler, L.; Carton, J.-P. *Macromolecules* **1992**, *25*, 2882.
(16) Turner, M. S.; Joanny, J.-F. *Macromolecules* **1992**, *25*, 6681.
(17) Pickett, G. T. *J. Chem. Phys.* **1996**, *104*, 1657.
(18) Solis, F. S.; Pickett, G. T. *Macromolecules* **1995**, *28*, 4307.
(19) Dobrynin, A. V.; Erukhimovich, I. Y. *Sov. Phys. JETP* **1991**, *53*, 570.
(20) Khoklov, A. R.; Nyrkova, I. A. *Macromolecules* **1992**, *25*, 1493.
(21) Benmouna, M.; Aziz, S.; Vilgis, T. A. *J. Polym. Sci., Part B* **1993**, *31*, 587.
(22) Nyrkova, I. A.; Khoklov, A. R.; Doi, M. *Macromolecules* **1994**, *27*, 4220.
(23) Solis, F. J.; Olvera de la Cruz, M. *J. Chem. Phys.* **1999**, *110*, 11517.
(24) Decher, G. *Science* **1997**, *277*, 1232.
(25) Milner, S. T.; Witten, T. A.; Cates, M. E. *Macromolecules* **1988**, *21*, 2610.
(26) Fleer, G.; Cohen-Stuart, M. A.; Scheutjens, J. M. H. M.; Cosgrove, T.; Vincent, B. *Polymers at Interfaces*; Chapman and Hall: London, 1993.

turbed from their Gaussian state, rather than elongated rods. For the blend to be overall electroneutral (a prerequisite for the A and B chains to be individually charged, but lacking small molecule countercharges) the following must obtain:

$$f\rho_A + (1 - f)\rho_B = 0 \tag{6}$$

To make contact with a convenient experimental scenario, we will choose to meet this condition by adjusting ρ_B. That is,

$$\rho_B = -\frac{f}{1-f}\rho_A \tag{7}$$

Essentially, keeping the properties of the A chains fixed, preparing a blend of a specific f requires adjusting the synthesis of just the B chains to have N monomers, each on average charged according to eq 7. Thus, the A chains can be drawn from a single large lot, while B chains can be synthesized to order.

At any rate, suppose the interaction of uncharged A and B monomers is characterized by a Flory−Huggins parameter χ. For definiteness, we shall define the local composition order parameter, ϕ, so that

$$\phi_A = f + \phi \tag{8}$$

$$\phi_B = (1 - f) - \phi \tag{9}$$

so that ϕ measures the local deviation of the volume fraction of A monomers from its average value and also measures the local *charge density*:

$$\rho_{es} \equiv e(\rho_A\phi_A + \rho_B\phi_B) = e\frac{1}{1-f}\rho_A\phi \tag{10}$$

where e is the elementary charge. Evidently, the mixed phase characterized by $\langle\phi\rangle = 0$ is charge-neutral, but any fluctuation in the distribution of A and B monomers induces an electrostatic charge separation. Here, angled brackets refer to a statistical average. Thus, the portion of the system free energy not dependent upon the chain conformations but dependent upon the field ϕ is

$$F[\phi] = \chi\phi_A\phi_B + \frac{1}{2\epsilon}\int d^3d^3r'\rho_{es}(r)G(r, r')\rho_e s(r') \tag{11}$$

which in Fourier space can be written as

$$F[\phi] = \text{const} - \chi\phi^2 + \frac{2\pi l_B{\rho_A}^2}{q^2(1-f)^2}\phi^2 \tag{12}$$

Note that the monomer size a is used here as the fundamental unit of length so that the wavevector $\vec{q}$ is dimensionless. The constant, l_B, is the Bjerrum energy,[28]

$$l_B = \frac{e^2}{kT\epsilon} \tag{13}$$

and is equivalent to the energy (in units of $kT = 1$) to bring two elementary charges to a distance $a = 1$ in the AB blend of dielectric constant ϵ. For simplicity in what follows (especially numerical work), we set $l_B = 1$, effectively setting the scale in which electric charge is measured. Thus, the effective potential coupling to fluctuations in ϕ, apart from those induced by chain connectivity and incompressibility, is

$$\alpha = -2\chi + \frac{4\pi{\rho_A}^2}{q^2(1-f)^2} \tag{14}$$

We can now proceed, in the usual manner, to determine the effect of chain connectivity and incompressibility.

While the disordered phase is characterized by $\langle\phi\rangle = 0$, fluctuations of ϕ about this value exist and can be directly measured in a scattering experiment:

$$\frac{1}{S_\phi(q)} = \frac{1}{fg_A(q)} + \frac{1}{(1-f)g_B(q)} + \alpha \tag{15}$$

which is the basic equation of the RPA.[27] Here, g_A and g_B are the scattering functions appropriate to each of the single chains A and B in the system. While it is appropriate to use the Debye function,

$$g(q) = 12\,\frac{Nq^2 + 6e^{-Nq^2/6} - 6}{Nq^4} \tag{16}$$

for both g_A and g_B, relatively simple (and, as we shall see below, accurate) results can be had from the Lorentzian approximation to the Debye scattering function:[27]

$$g_A(q) = g_B(q) = \frac{N}{1 + Nq^2/12} \tag{17}$$

The Lorentzian scattering function is an interpolation between the high-q self-similar scattering of a random walk in three dimensions and the low-q scattering of N uncorrelated objects.[29] Using eq 17, defining $x \equiv Nq^2$ and $Q_A \equiv \rho_A N$, the total charge on the A chain, the full collective scattering function can be written as

$$S_\phi(x) = \frac{12(1-f)^2 fNx}{(1-f)x(12+x) + 48f\pi Q_A - 24\chi f(1-f)^2 Nx} \tag{18}$$

This scattering function is characterized by a peak away from $x = 0$, indicating that fluctuations of the homogeneous phase are characterized by a length scale:

$$x_{max} = 4\sqrt{3\pi}\sqrt{\frac{f}{1-f}}\,Q_A \tag{19}$$

and the scattering at this peak amplitude diverges when

$$S_\phi(x = x_{max}) = \infty \rightarrow \chi_{spin}N = \frac{1}{2f(1-f)} + \sqrt{\frac{\pi}{3f(1-f)^3}}\,Q_A \tag{20}$$

As in the diblock case,[30] x_{max} is not a function of χ. Thus, for a neutral, symmetric blend, $\chi N = 2$ is the location of the macrophase instability of the homogeneous blend, but the presence of charges serves to put off the instability to higher and higher values of χN, linearly with the amount of charge on the A chain. For symmetric blends, $f = 1/2$, the spinodal occurs at

(27) deGennes, P.-G. *Scaling Concepts in Polymer Physics*; Cornell University Press: Ithaca, 1979.

(28) Grossberg, A. Y.; Khokhlov, A. R. *Statistical Physics of Macromolecules*; American Institute of Physics: New York, 1994.

(29) Marques, C. M.; Fredrickson, G. H. *J. Phys II France* **1997**, *7*, 1805.

(30) Leibler, L. *Macromolecules* **1980**, *13*, 1602.

$$\chi_{spin}N = 2 + 4\sqrt{\frac{\pi}{3}}Q_A \approx 2 + 4.09Q_A \qquad (21)$$

Alternatively, the full q-space dependence of the full Debye function can be used numerically to locate the divergence of the full scattering function. A comparison between the Debye and the approximate result is shown in Figure 1, as well as a comparison to SCF calculations on the $f = 1/2$ blend as carried out below, and these results are consistent with the analysis given in refs 20−22. While it is certainly possible to go beyond a linear stability analysis of the uniform field,[30] this will be sufficient for the purpose of validating the numerical SCF calculations below.

The presence of charge not only delays the decomposition of the blend but more importantly rules out a structureless $x_{max} = 0$ phase separation.[20] Mesophases are required.

3. Strong Segregation Spherical/Cylindrical Unit Cell

The strong segregation limit[5] of this system is equally straightforward to analyze. The lamellar phase is characterized by planar slabs of uniformly charged fluid, ρ_A, alternating with slabs of fluid with a charge ρ_B. The AB interface is characterized by an interfacial tension γ. Keeping ρ_A fixed as above, there are two cylindrical phases to consider, one where the A fluid is in the interior of the cylindrical domains and the B fluid forms an exterior corona and one in which the B phase is on the interior and the A phase is on the exterior. Similarly, there are two spherical phases, one composed of A cores and a B corona and one where the A fluid forms the corona and the B fluid is in the core.

In the lamellar phase, we set up a coordinate system which has as its origin the midpoint of a particular A domain, and r is the coordinate along the slab normal. The AB interface is located at $r = R_A$, and the midpoint of the adjacent B domain is located at r_{tot}. Thus $r = 0$ and $r = r_{tot}$ are chosen to be planes at which the internal electric field, $\vec{E}$, vanishes. Consequently, we can focus on just the properties of this half-layer. Using $\vec{E}(r = 0) = 0$, an elementary application of Gauss' law implies that

$$E_r(r) = 4\pi\rho_A r \qquad \text{when } 0 < r < r_A \qquad (22)$$

and that in the B domain

$$E_r(r) = 4\pi \frac{f}{1-f}\rho_A(r_{tot} - r) \qquad (23)$$

where

$$r_A = f r_{tot} \qquad (24)$$

ensures overall electroneutrality in the layer (that is, the amount of charge enclosed in a Gaussian pillbox extending from $r = 0$ to $r = r_{tot}$ is $Q/l^2 = \rho_A r_A + \rho_B(r_{tot} - R_A)$ using eq 7). Now it is a simple matter to calculate the electrostatic self-energy of this layer:

$$F_{es} = \frac{1}{8\pi}\frac{\int_0^{r_{tot}} \vec{E}\cdot\vec{E}}{r_{tot}} \qquad (25)$$

$$= \frac{2}{3}\pi f^2 \rho_A^2 r_{tot}^2 \qquad (26)$$

Similarly, the surface energy per unit volume is

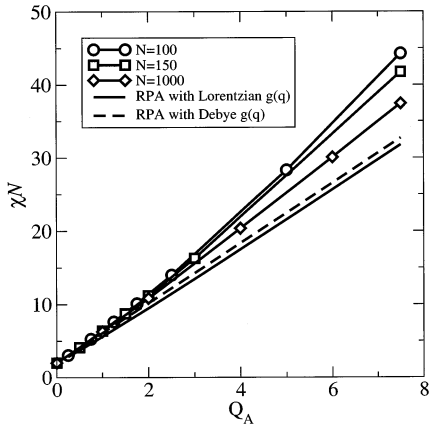

Figure 1. Symmetric phase spinodal. The symmetric $f = 1/2$ blend spinodal as calculated in the RPA for both the Debye (dashed) and Lorentzian (solid) scattering functions is shown. Also, SCF results on $N = 100$, 150, and 1000 are shown for the transition from the disordered to the lamellar phases. There is general agreement between the treatments, although a systematically higher interaction parameter is required in the SCF treatment, a trend which diminishes at higher and higher N.

$$F_{surf} = \frac{\gamma}{r_{tot}} \qquad (27)$$

so that the total free energy in the lamellar phase is

$$F_{lam}[r_{tot}] = F_{surf}[r_{tot}] + F_{es}[r_{tot}] \qquad (28)$$

where the equilibrium size of the lamellar repeating pattern, r_{tot}, is determined by $\partial r_{tot} F_{lam} = 0$:

$$r_{tot}^{eq} = \left[\frac{3\gamma}{4\pi f^2 \rho_A^2}\right]^{1/3} \qquad (29)$$

The equilibrium free energy per unit volume of the lamellar phase is

$$F_{lam}^{eq} = 3^{2/3}2^{-1/3}\pi^{1/3} f^{2/3}\gamma^{2/3}\rho_A^{2/3} \qquad (30)$$

In the sharp-interface limit, with a virtually complete segregation of A and B fluids into separate domains, eq 30 is exact.

The cylindrical and spherical phases, however, can only be approximated by a "single domain" calculation like in the lamellar case.[12,31] Here, the packing of cylindrical domains onto a hexagonal lattice requires a 6-fold rotational symmetry of the single domain. We will approximate this packing effect by assuming that the cylindrical domains are *exactly* circular in cross section and that the spherical domains are *exactly* spherically symmetric. This "spherical−cylindrical" unit cell approximation can be relaxed in more dependable numerical methods, such as those carried out below, but for the purposes of determining the low-temperature, and hence high χN, behavior, the present treatment is sufficient.

Thus, when A monomers form the core of a cylindrical domain, let r stand for the distance from the axis of cylindrical symmetry, and let r_A be the radius of the A-filled core. The overall size of the cylinder is r_{tot}, and overall neutrality of the cylindrical domain requires that

(31) Vavasour, J. D.; Whitmore, M. D. *Macromolecules* **1992**, *25*, 5477.

$$\rho_A {r_A}^2 + \rho_B({r_{tot}}^2 - {r_A}^2) = 0 \rightarrow r_A = r_{tot}\sqrt{f} \quad (31)$$

so that the electric field is always oriented in the $\hat{r}$ direction with a magnitude

$$E(r) = 2\pi\rho_A r \qquad \text{when } 0 < r < r_A \quad (32)$$

$$E(r) = 2\pi \frac{f}{1-f}\rho_A \frac{{r_{tot}}^2 - r^2}{r} \qquad \text{when } r_A < r < r_{tot} \quad (33)$$

The electrostatic contribution to the free energy per unit volume can then be calculated:

$$F_{es} = \frac{1}{8\pi}\frac{\int_0^{r_{tot}} 2\pi r\, dr \vec{E}\cdot\vec{E}}{\pi {r_{tot}}^2} \quad (34)$$

$$= \frac{\pi f^2 {\rho_A}^2 {r_{tot}}^2}{2(1-f)^2}(f - 1 - \log f) \quad (35)$$

Together with the correct surface energy term,

$$F_{surf} = \frac{\gamma 2\pi r_A}{\pi {r_{tot}}^2} = \frac{2\gamma\sqrt{f}}{r_{tot}} \quad (36)$$

the overall free energy depends on the unknown r_{tot}, which can then be fixed through minimizing. In this way, the overall size of the cylindrical domains can be found in equilibrium:

$$r_{cyl}^{eq} = \frac{2^{1/3}(1-f)^{2/3}\gamma^{1/3}}{\pi^{1/3} f^{1/2} {\rho_A}^{2/3}(1 - f + \log f)^{1/3}} \quad (37)$$

and the overall cylindrical energy with A cores becomes

$$F_{cyl}^{A-in} = \left(\frac{\pi}{2}\right)^{1/3} \frac{3f\gamma^{2/3}{\rho_A}^{2/3}}{(1-f)^{2/3}}(f - 1 - \log f)^{1/3} \quad (38)$$

In a similar manner, the equilibrium free energies of the other phases can be similarly calculated:

$$F_{cyl}^{A-out} = 3\left(\frac{\pi}{2}\right)^{1/3}\gamma^{2/3}{\rho_A}^{2/3}(1-f)^{1/3}(-f - \log(1-f))^{1/3} \quad (39)$$

$$F_{sphere}^{A-in} = 3^{5/3}\pi^{1/3}10^{-1/3}\gamma^{2/3}{\rho_A}^{2/3} f\,(2 + f^{1/3})^{1/3} (1 + f^{1/3} + f^{2/3})^{-2/3} \quad (40)$$

$$F_{sphere}^{A-out} = 3^{5/3}\pi^{1/3}10^{-1/3}\gamma^{2/3}{\rho_A}^{2/3}(1-f)^{1/3} (3(1-f)^{1/3} + f - 3)^{1/3} \quad (41)$$

In Figure 2, we show the relative stability of each of these phases. As each of these free energies scales in exactly the same way with γ and ρ_A, the phase boundaries are solely a function of the overall composition of the blend, f. The ordering of the phases is found to be

Spheres, A core when $0.000000 < f < 0.215252$ (42)

Cylinders, A core when $0.215252 < f < 0.354992$ (43)

Lamellar when $0.354992 < f < 0.645008$ (44)

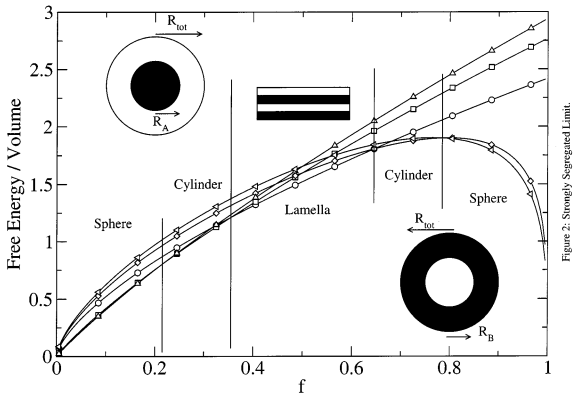

Figure 2. Strongly segregated limit. Here are results on the strongly segregated system, characterized by sharp interfaces and complete segregation of the A and B polymers. As a result of the asymmetry in the defined quantities, that is, ρ_A is held constant while ρ_B is used to enforce overall electroneutrality, the free energies are not symmetric about $f = 1/2$, although the actual phase boundaries *are symmetric*.

Cylinders, B core when $0.645008 < f < 0.784748$ (45)

Spheres, B core when $0.784748 < f < 1$ (46)

Thus, the trivial strongly segregated model gives very similar phase boundaries to those of the classical diblock phases. The next question is, how do the strongly segregated and the linear stability calculations above merge together for realistic values of the degree of segregation χN, the degree of charge ρ_A, and polymer molecular weight N? Thus, we turn to numerical lattice calculations, relaxing all assumptions concerning the shape of the domains up to a requirement that the mesophases display translational invariance in one direction.

4. SCF Method

The method we choose to implement here is that of Scheutjens and Fleer,[26] as generalized to a two-dimensional lattice.[32] While off-lattice calculations are certainly possible[5,9] and perhaps superior, the advantage of the lattice formalism over those based on an effective diffusion equation describing the self-consistent polymer conformations is that the lattice formalism inherently captures the *finite extensibility* of physical chains, while asymptotically capturing the random-walk statistics of off-lattice Gaussian chains. Thus, we can expect the lattice method we use here to be more sensitive to finite molecular weight effects which are completely absent from, for example, the RPA calculations above. That is, finite, though long, chains are not *exactly* described by a Debye function, as the molecular weight dependence of the AB interfacial tension, γ, indicates.

So, we shall proceed as above to consider a blend of A and B type chains, each of molecular weight N, each of which has a uniformly distributed electric charge, ρ_A per monomer on the A chains and ρ_B per monomer on the B chains. Using f as the overall fraction of the system taken up by A monomers in this *incompressible* treatment, the average lattice occupation by B monomers must be $(1 - f)$. Overall electroneutrality is enforced by eq 7.

It is a simple matter on a lattice to build up all the statistics of the A chains given the local chemical potential $U_A(y, z)$ giving the free energy cost to insert an A monomer

(32) Huang, K.; Balazs, A. C. *Phys. Rev. Lett.* **1991**, *66*, 620.

at the lattice position (y, z):

$$U_A(y, z) = \alpha(y, z) + \chi\langle\phi_B\rangle(y, z) + \rho_A\Phi_{es}(y, z) \quad (47)$$

Here, α is a self-consistently determined potential, the same for both A and B monomers which is adjusted so that $\phi_A(y, z) + \phi_B(y, z) = 1$, that is, so that incompressibility is maintained. The angled brackets above refer to the "contact fraction" giving the average number of B monomers which are nearest neighbors to a test A monomer inserted into the site (y, z). The final term accounts for all electrostatic interactions. Given an arrangement of A and B monomers, the local charge density is

$$\rho_{es} = \rho_A\phi_A + \rho_B\phi_B \quad (48)$$

so that the electorstatic potential is

$$\Phi_{es} = \sum_{y,z,y',z'} \rho_{es}(y, z)G^{lattice}(y, z, y', z')\rho_{es}(y', z') \quad (49)$$

where the operator $G^{lattice}$ satisfies a *discretized* version of the normal electrostatic Green's function:

$$\nabla_{lattice}{}^2 G^{lattice} = 4\pi\delta_{y,y'}\delta_{z,z'} \quad (50)$$

Here, the discrete Laplacian operator we have chosen to *lowest order* is the familiar 5-point discrete operator:[33]

$$\nabla_{lattice}{}^2\mu(y, z) = \mu(y + 1, z) + \mu(y - 1, z) + \mu(y, z + 1) + \mu(y, z - 1) - 4\mu(y, z) \quad (51)$$

where μ is any quantity of interest which varies from one point of the lattice to another. As implemented on a finite lattice, this operator necessarily operates on quantities outside the lattice dimensions set at L_y and L_z, so the operator must be supplemented with boundary conditions. In all that follows, we apply reflecting boundary conditions at each of the boundaries of the lattice, so that all quantities will obey

$$\mu(y, L_Z + 1) = \mu(y, L_Z) \quad (52)$$

$$\mu(y, 0) = \mu(y, 1) \quad (53)$$

and so on. By solving eq 50, subject to boundary conditions as in eq 53, numerically (essentially the inversion of a linear operator), the electrostatic contribution to the A monomer potential can be calculated, eq 47, as well as the electrostatic contribution to the overall per-site system free energy:

$$F_{es} = \frac{1}{2}\sum_{y, z}\rho_{es}(y, z)\Phi_{es}(y, z) \quad (54)$$

Given this approximate treatment of electrostatics, the full self-consistent program can be carried out, whereby initial guesses for both U_A and U_B allow the calculation of both ϕ_A and ϕ_B, which can then be used to further refine the initial guesses for U_A and U_B until incompressibility is achieved and eq 47 is satisfied for both A and B monomers. In practice, a configurational tempering scheme is used,[9] whereby at each combination of f, ρ_A, L_Z, and L_Y a number of random initial guesses for U_A and U_B are made (between 5 and 10), a self-consistent solution is determined, and the lowest free energy conformation is retained for reporting. In this manner, equilibrium phase diagrams of the disordered−cylindrical−lamellar phases can be constructed as in the next section.

(33) Press, W. H.; Teukolsky, S. A.; Vetterling, W. T.; Flannery, B. P. *Numerical Recipes in C*; Cambridge University Press: Cambridge, U.K., 1992.

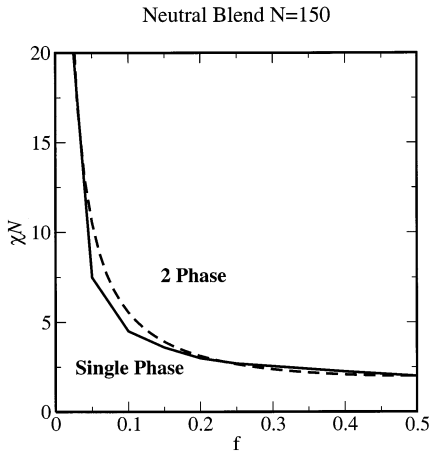

Figure 3. Neutral blend. For $0 < f < 1/2$, the single and two-phase regions as determined by the SCF lattice calculations are presented when $\rho_A = 0$, as compared to the RPA calculation (dotted line) for $N = 150$. The configurational tempering procedure used here introduces statistical uncertainty into the phase boundaries as determined by the SCF. However, the degree of accuracy is ample to determine broadly the trends when the chains in the blend carry electric charges.

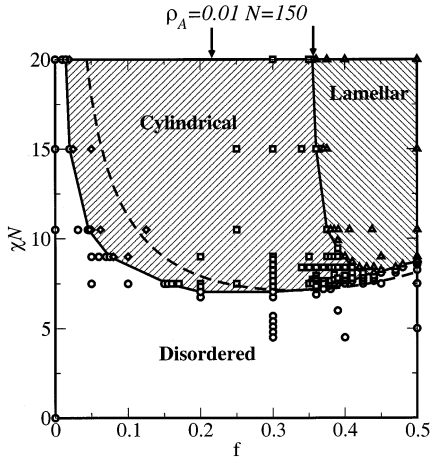

Figure 4. Charged blend, $Q_A = 1.5$, $N = 150$. Here, the A and B chains each have $N = 150$ and the A chains are held with $\rho_A N = 1.5$. The cylindrical, lamellar, and disordered phases are shown. The two-dimensional lattice calculation used here is incapable of determining the cylinder−sphere transitions. The two arrows at the top of the diagram indicate the strong segregation limit transition points for the sphere−cylinder and the cylinder−lamella transitions. The dashed line indicates the spinodal of the disordered phase as determined in the RPA calculation with the Lorentzian scattering function. The symbols indicate individual combinations of f and χN used to determine phase boundaries.

5. Results

The main results are contained in Figures 3−5, where in the strictly *two-dimensional* lattice model we have determined the stability of three of the classical phases that exhibit translational symmetry along at least one axis. Thus, we are limited to dealing with the disordered, cylindrical, and lamellar phases, although there are certainly methods which would allow the spherical packed phase (and indeed more complex bicontinuous phases) to be included. To make as few assumptions as possible, for

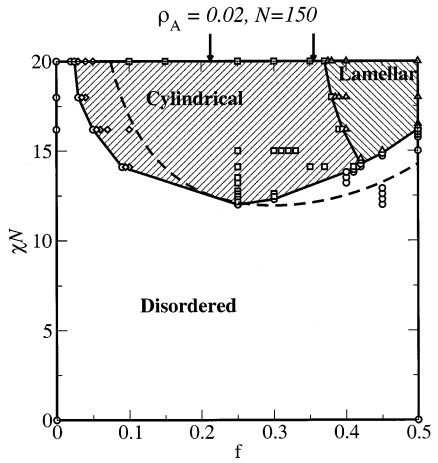

Figure 5. Charged blend, $Q_A = 3.0$, $N = 150$. Here, the A and B chains each have $N = 150$ and the A chains are held with $\rho_A N = 3$. Symbols, lines, and figures are as in Figure 4. Clearly charge serves to compatibilize the blend as well as to introduce composition (and charge) modulations.

each value of χN, f, and ρ_A (equivalently Q_A) we have made a scan through various lattice sizes, with $L_y = 1, ..., 30$ and $L_z = 1, ..., L_y$, and at each of these 465 unique combinations of L_y and L_z, we have executed between 5 and 10 calculations with independent random initial guesses for the monomer potentials, eq 47. We retain the converged solution with the lowest free energy and visually inspect the volume fraction profiles to make a determination of morphology. The symbols shown in Figures 4 and 5 represent individual determinations of this type of the thermodynamic ground state. Furthermore, the phase diagram with $\rho_A = 0$, Figure 3, shows the typical errors incurred in the phase boundaries using this configurational tempering method, as this situation applies to a simple binary blend, so the RPA calculation of the spinodal should lie entirely *within* the two-phase region. We note that the macroseparation instability at $\chi N = 2$ for the symmetric $f = 1/2$ neutral blend is correctly achieved.[27]

In all cases, the essential symmetry of the system implies that the mean-field critical point should occur at $f = 1/2$. To determine the actual nature of the transition near $f = 1/2$ (almost certainly a fluctuation-induced first-order transition[19]) is not the focus of this work. Indeed, it is observed that the cylindrical phase does not extend to the critical point. On the other hand, the calculations extend to the strong segregation limit, as seen by the fact that the lamellar−cylinder transition (marked by the arrows) is achieved for $\chi N = 20$.

In Figure 4, it is seen that the order−disorder point for the symmetric blend is shifted toward a higher value of approximately $\chi N = 7.5$, as compared to 7.2 as predicted by the RPA calculation (eq 21 when $Q_A = 1.5$ and $N = 150$). The dashed line corresponds to the RPA prediction for the linear stability limit of the homogeneous, single-phase region of this diagram. There is, admittedly, only a rough correlation between the RPA prediction and the results of this lattice calculation. The strongly segregated limit of the cylinder−lamellar transition is also roughly obeyed. The phase boundaries of eqs 43−46 are indicated by the two arrows at the top of the figure. The cylinder−sphere boundary has been shown, although the calculations we have executed are incapable of describing the spherical phase on the same footing as the cylindrical phase (that is, in a lattice of the same geometry, with the same interactions; a quasi-one-dimensional lattice calculation in the spherical unit cell approximation is certainly feasible, but hardly in keeping with our desire to keep the assumptions surrounding the SCF calculations as few as possible).

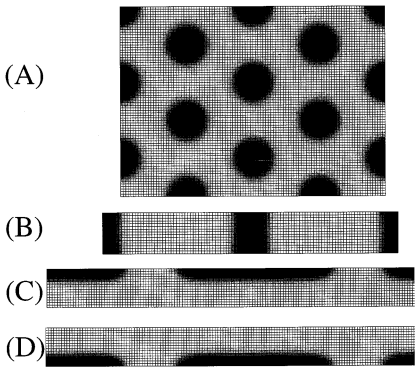

Figure 6. Thin films. (A) For $N = 150$, $f = 1/4$, and $Q_A = 1.5$, the bulk phase is cylinders hexagonally packed, seen here in cross section. Also evident is the resolution of the lattice. High density of A monomers is indicated by dark shading. (B) For the same parameters as in (A), the lattice has been modified so that the lower surface is electrically grounded, and the upper surface is insulating, appropriate to a thin film cast on an electrode. Both the upper and lower surfaces are neutral with respect to surface energies. (C) The electrode in (B) is now held at an elevated potential, of magnitude $\Phi_{es} = 0.05$. The A monomers are driven away from the electrode but still make a useful pattern at the upper (insulating) surface. (D) As in (C), but now $\Phi_{es} = -0.05$, so that the A monomers are drawn toward the electrode.

The rough scenario is certainly borne out, however. The presence of "compatibilizing" charges delays significantly the phase separation, and when the phase separation occurs, it is characterized by mesoscopic order. Macroscopic phase separation has *never* been observed in these calculations to be the thermodynamic state.

As in Figure 5, when the charge per chain doubles, the mesoscopic order occurs at ever more elevated values of χN. Again, the dashed line gives the comparison to the RPA calculation on the spinodal of the disordered phase. In this case, an even larger discrepancy between the RPA and SCF calculations is exhibited. As in Figure 1, the discrepancy diminishes at small Q_A and large N, indicating that molecular weight enters the SCF theory in a nonuniversal manner that nevertheless reproduces the correct scaling behavior at large molecular weight.

In addition to surveying the bulk equilibrium phases, a sensitivity to external fields and boundary conditions is evident in Figure 6. In the upper panel (A) is the bulk morphology for the blend under consideration, $Q_A = 1.5$, $N = 150$, and $f = 0.25$. The next panel (B) shows the same film, but now confined into a film of thickness $L_Z = 15$ lattice units, corresponding to the bulk semirepeat spacing of the bulk hexagonal phase. This film is grounded along its lower $z = 1$ boundary and insulating along its upper $z = 15$ boundary. Thus the calculation is relevant to the thin blend film cast on a metal-coated substrate and has a distinctly different morphology from the kinetically ordered layer-by-layer assembled films.[24] The hexagonal phase is destabilized, and a bridging striped conformation occurs. When the metallic surface in (B) is raised in electrostatic potential (C) or lowered (D) by only 0.05 (so that a single charge would gain an energy equivalent to 0.05 kT in traversing the film), the morphology of the pattern changes drastically. Fully exploring the consequences of this external control will be an interesting direction for further study, with the aim of gaining nanometer control of the patterns with externally applied electric fields.[38]

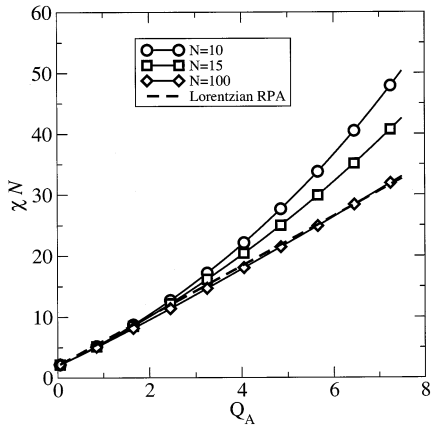

Figure 7. Approximate Laplacian RPA. When the Laplacian operator is replaced by its lattice approximant, finite molecular weight effects are present similar to the ones in Figure 1.

Clearly, these charged blends readily form patterns, and the patterns can be dramatically affected via external triggers.

6. Discussion

The most interesting discrepancy between the RPA and SCF calculations is the molecular-weight-controlled effect in Figure 1. In the RPA formulation, molecular weight enters the theory as (1) the overall magnitude of the scattering function, (2) controlling the radius of gyration of the disordered coils, and (3) setting the overall charge per A chain. In the SCF calculation, however, once the scaled units of the RPA have been used, there is still not a collapse of the data with differing N's. Part of the reason is surely that even $N = 100$ walks on a square lattice have significantly different scattering functions (with an anisotropy which falls as $1/N$) from Gaussian chains. But another source of error enters the SCF calculations, in that the Laplacian operator has been approximated discreetly, so that its Fourier transform is

$$\nabla^2 \rightarrow 2(1 - \cos q_y) + 2(1 - \cos q_z) \qquad (55)$$

so that

$$\nabla^2 \rightarrow -(q_y^2 + q_z^2) \qquad (56)$$

is only satisfied for small q_y, q_z. The RPA, of course, uses the correct form for the G_{es} interaction propagator (essentially the functional inverse of the Laplacian, $-1/q^2 \rightarrow \delta(\vec{r})$ in three dimensions). So, using

$$\alpha = -\chi + \frac{4\pi\rho_A^2}{(1 - \cos q_z^2)(1 - f)^2} \qquad (57)$$

in eq 15, the location of the instability can be determined numerically. Instantly, however, it is clear that Q_A is not the scaling variable that it appears to be, so RPA-like scaling will occur only when the relevant $\vec{q}$ range corresponds to distances much larger than the chain radius of gyration. Figure 7 shows the results of such a calculation, indicating that the finite-N effects present in Figure 1 and Figures 4−5 are in fact artifacts of the manner in which we have calculated the electrostatic portion of the free energy. The numerical RPA executed with the approximate Laplacian admittedly does not display quantitative agreement with the SCF results of Figure 1, although the manner in which the discrepancy grows with Q_A is qualitatively consistent.

The self-assembled patterns created by diblock melts are indeed quite impressive but are limited in their practical applications to nanoscopic length scales. This is indeed an advantage for many applications, such as making and controlling templates for nanomagnetic storage solutions. But other applications, such as creating photonic band gap materials, require self-assembled patterns on a much larger length scale.[34] While the length scale of diblock patterns grows with molecular weight, $L \approx N^{2/3}$,[13,14] so in principle any particular length scale pattern can be attained through synthesizing large enough N copolymers, the practical limits of processability and large-scale, well-controlled synthesis rule out creating 10 μm patterns. In the present case, however, the ultimate length scale of the pattern, eq 19, is controlled by the combination of $Q_A = \rho_A N$. Thus, diblocklike patterns on *any* length scale can be conveniently created via designing the precise amount of charge on the chains. To be most useful in this context requires the limit of lightly charged chains and therefore incompatibility parameters with $\chi N \approx 2$. In this limit, polydispersity in the chains will induce only a small correction to the phase diagrams as calculated, as the phase-separated domains in any of the weak through strongly segregated limits will contain very many chains, with the pattern scale much larger than an individual chain radius of gyration. The opposite limit, with very highly charged chains segregated into very small, perhaps single-chain-sized, domains, is interesting to contemplate and is a limit where polydispersity will have its biggest influence.

Another advantage to this system is that much work has already been done on the model in eq 2.[10] This work is usually meant to give qualitative results for an equivalent *copolymer* system. Work based on this model, however, is directly related to the electroneutral blend we consider here. For example, the effect of an oscillatory shear on the alignment of the lamellar domains in the charged blend has been determined.[35] The effect of the charged blend as a compatibilizer for the *uncharged* AB blend has been calculated.[36] Confinement and surface interactions have been considered as affecting the orientation of lamellar domains in thin films.[37] Each of these problems, while qualitatively describing block copolymer systems, more or less exactly describes the current system, up to a finite molecular weight effect such as is evident in Figure 1.

Then again, as the composition pattern necessarily entails a spatial separation of charges, these patterns could be amenable to applications and controls for which diblocks are not suitable. The control of thin film diblock patterns via an external electric field coupling to a differential in the A and B material polarizability has been demonstrated clearly,[38] but the strength of the effect should be even more pronounced when the external field couples to a real charge distribution. A striking qualitative difference exists between the behavior of a charged pattern versus a pattern in polarizability. In using electric fields to orient thin-film domains of block copolymers, it is readily found that the striped pattern follows *the electric field lines*. As in

(34) Subramanian, G.; Manoharan, V. N.; Thorne, J. D.; Pine, D. J. *Adv. Mater.* **1999**, *11*, 1261.
(35) Drolet, F.; Chen, P.; Vinals, J. *Macromolecules* **1999**, *32*, 8603.
(36) Huang, C.; Olvera de la Cruz, M.; Swift, B. W. *Macromolecules* **1995**, *24*, 7996.
(37) Podariu, I.; Chakrabarti, A. *J. Chem. Phys.* **2000**, *113*, 6423.
(38) Morkved, T. L.; Lu, M.; Urbas, A. M.; Ehrichs, E. E.; Jaeger, H. M.; Mansky, P.; Russell, T. P. *Science* **1996**, *273*, 931.

Figure 6, when the pattern is composed of phase-separated charge layers, the pattern has a tendency to follow the *equipotential surfaces*. Finally, the existence of a static electric field in the layer would be very important in creating thin-film polymer diodes.[39]

Creating blends of oppositely charged polymers is apt to require experimental ingenuity. Weak polyacids, or even traditionally polyelectrolytes, are accompanied in their synthesis by small molecule neutralizing counterions. The applications we envision here require that the counterions can be at least partially removed permanently from the system. A physical manifestation of this system would be a disassociated (and therefore high-temperature) ionomer melt or an ionomer melt with correspondingly weakened electrostatic interactions. Steric effects can be used to weaken the electrostatic coupling by disallowing intimate contact between the physical charges.

(39) deMello, J. C.; Halls, J. J. M.; Graham, S. C.; Tessler, N.; Friend, R. H. *Phys. Rev. Lett.* **2000**, *85*, 421.

7. Conclusions

Electroneutral blends of oppositely charged polymers have been examined in three complementary and consistent formalisms. Calculations in the RPA, in the strongly segregated limit, and with a numerical lattice SCF all indicate that these blends will form complex three-dimensional patterns in thermodynamic equilibrium. The electrostatic analogy that has been used for many early and some current approximate treatments of block copolymers has in this instance been taken literally. Thus, the electroneutral blend of copolymers has many of its features already known as a byproduct of much work on the diblock system. The patterns are characterized by a nonuniform distribution of electric charge and hence are amenable to control with external electric fields.

Acknowledgment is made to the donors of the Petroleum Research Fund, administered by the American Chemical Society, for support of this research.

LA026465F